Brushing-Assisted Two-Color Quantum-Dot Micro-LED Array Towards Bi-Directional Optogenetics

Dacheng Mao, Zheshun Xiong, Matthew Donnelly, and Guangyu Xu, *Member, IEEE*

***Abstract*— Bi-directional optogenetics at single-cell level requires localized, bright, and multi-color light sources to activate both excitatory and inhibitory opsins. To this end, here we report a simple fabrication method of high-density, two-color, quantum dot (QD) based micron-sized light emitting diode (micro-LED) arrays. In particular, we micro-patterned InP/ZnS QDs on top of GaN-based micro-LED pixels via a simple brushing method, and coated them with a spectral filter. The resulting array featured sub-20 μm sized light spots near both 462 nm and 623 nm, with their optical power density being *ca.* 0.1 – 1.0 mW/mm^2. Combined with its low crosstalk and fast response, our two-color QD-LED array may hold promise for bi-directional optogenetics ultimately at the cellular level.**

***Index Terms*— Multi-color micro-LED array, bi-directional optogenetics, micropatterning of quantum dots.**

I. Introduction

BI-DIRECTIONAL optogenetic modulation of neural activity is an emerging method to identify the linkage between cell connectivity and animal behavior [1]–[3]. In this method, neurons are expressed with light-sensitive opsins, thereby their activities can be either excited or inhibited upon patterned light illumination in a temporally precise and cell-type specific manner. While the former functionality (excitation) can also be achieved by other methods, the latter (inhibition) may find its unique use in developing therapy for neurological disorders (e.g., epilepsy) [4].

To achieve precise optogenetic modulation ultimately down to cellular precision, micron-sized light emitting diodes (i.e., micro-LEDs) have been recognized for their scalability, good lifetime, and medium power dissipation [5]–[8]. In particular, these devices can be built into a high-density array to achieve optogenetic control of individual cells [7], [8]. To extend their usage for bi-directional optogenetics, it will be essential to examine if such micro-LED arrays can be engineered to output multiple wavelengths (i.e., multi-color) with their optical power density being *ca.* 0.1 – 1.0 mW/mm^2, which can then serve to activate both excitatory and inhibitory opsins (e.g., *ChR2* and *Halo* [2], [3], [9]–[11] *or ChRmine* and *Mac* [11]–[13]).

To date, multi-color micro-LED arrays have been built from III-V quantum wells, organic films, nanocolumns, phosphors, or quantum dots (QDs) [14]–[18]. Among them, III-V and phosphor based arrays are noted for their high brightness and quantum efficiency [14], [17], but often built in large pitches (>20 μm) [19]. On the other hand, organic and nanocolumn LEDs have been placed in dense arrays [15], [16], but yet to achieve high brightness and color purity for bi-directional optogenetics.

To this end, QD-based arrays have been noted for their color saturation, stability, light power density, spectral tunability, and compatibility with complementary metal-oxide semiconductor based processes [19]–[21]. These arrays can emit light at targeted wavelengths based on either electroluminescence (EL) or photoluminescence (PL) from micro-patterned QDs, which have established their use in display applications [19], [21]. While the former has been suggested for photomedical applications [22], the latter can be made in a small pitch [18] to offer high-resolution illumination at the cellular level. Both of them, however, often involve complex fabrication steps such as transfer printing, layer-by-layer assembly, or ink-jet printing [23]–[27]. It may thus prove beneficial to develop cost-effective alternative methods to build these QD-LED arrays.

Here we present a 17-μm pitched two-color QD-LED array based on brushing-assisted micropatterning of InP/ZnS QDs, aiming to enable bi-directional optogenetics at the cellular level. Our QDs were patterned on top of GaN-based LED pixels by polydimethylsiloxane (PDMS) assisted brushing steps, serving as a simple, cost-effective approach of QD patterning compared to existing methods [23]–[27]. We then coated the array with a photoresist-based spectral filter, which yielded reduced spectral crosstalk and improved optical power densities of LED pixels compared to distributed-Bragg-reflector based filters [28]. The resulting array featured sub-20 μm sized light spots near both 462 nm and 623 nm, with their optical power density being *ca.* 0.1–1.0 mW/mm^2. The light-conversion efficiency of our QDs was *ca.* 5%, on par with prior PL-based QD-LEDs [27], [29]. Combined with its low crosstalk and fast response, our two-color QD-LED array manifests its promise for bi-directional optogenetic studies at the cellular level.

II. Methods

We first fabricated a GaN-based blue micro-LED array that can output 462/19 nm light as we reported before [7]. The LED

AQ:1 Manuscript received August 11, 2021; accepted August 25, 2021. This work was supported by the National Science Foundation under Grant ECCS-1835268, Grant ECCS-2046031, and Grant ECCS-2055457. The review of this letter was arranged by Editor D. Kuzum.

AQ:2 *(Corresponding author: Guangyu Xu.)*

AQ:3 The authors are with the Department of Electrical and Computer Engineering, University of Massachusetts Amherst, Amherst, MA 01003 USA (e-mail: guangyux@umass.edu).

Color versions of one or more figures in this letter are available at https://doi.org/10.1109/LED.2021.3108554.

Digital Object Identifier 10.1109/LED.2021.3108554

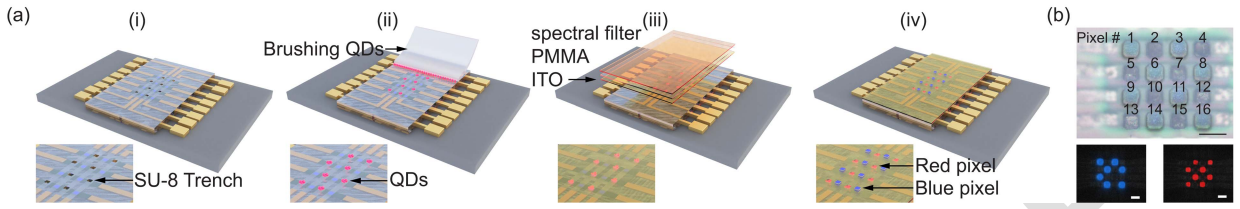

Fig. 1. **Array Fabrication**. (a) Illustrations (insets are zoom-in views) of the QD-LED array at each fabrication step. A PDMS piece was used to brush QDs into 8 SU-8 trenches on a passivated GaN-based micro-LED array (i) to form the red pixels (ii). The QD-patterned array was then covered by ITO/PMMA/spectral layers (iii), followed by opening the regions of 8 blue pixels (iv). (b) The optical image (top) and working status (bottom) of the fabricated QD-LED array. In the latter, pseudo-colored fluorescence images of 7 blue (bottom left) and 8 red (bottom right) pixels are overlaid together with the array image. Each working blue [red] pixel was individually illuminated (biased at $I_{LED} = 6\ \mu$A); the corresponding fluorescence image was captured with a 400 [565] nm long pass dichroic mirror plus a 460/50 [605/70] nm emission filter. Scale bar, 20 μm.

pixels, each 7.8 μm-by-7.8 μm in size, were patterned in a 4-by-4 crossbar structure with a 17 μm pitch and passivated with a plasma-enhanced chemical vapor deposition based SiO_2 layer (~200 nm). To build a two-color array, we next patterned 9.7 μm-by-9.7 μm sized, 7 μm-deep, SU-8-based trenches over 8 pixels of the array (Fig. 1(a)(i)). These trenches would later be filled with QDs, which can convert the blue light illumination from LED pixels to a red-shifted light via PL.

We then added one drop of toluene mixed with 25 mg/mL InP/ZnS QDs that can emit at 623/45 nm (Mesolight Inc) to the SU-8 surface over the array; the toluene solvent was found to naturally evaporate in ambience within *ca.* 1 min, drying QDs on the SU-8 surface. After that, we immersed the array in acetone where QDs were found to be rewetted (i.e., partially resuspended). We were then able to physically brush QDs into SU-8 trenches with a PDMS piece. This simple step worked effectively in 1) filling QDs into those trenches, possibly because the density of QDs is higher than that of acetone (Fig. 1(a)(ii)); and 2) cleaning the QD residue left on the SU-8 surface during the drying step. We then named these 8 QD-coated pixels as red pixels and the remaining 8 pixels (not coated with QDs) as blue pixels.

To improve the color purity of 8 red pixels, we next coated them with a spectral filter to block the blue illumination from the LED pixels beneath QDs (Fig. 1(a)(iii)). To achieve this, we first sequentially formed a sputtered indium tin oxide (ITO) layer (~500 nm) and a spin-coated PMMA layer (~600 nm) on the QD-LED array to passivate the filled QDs. Such stacked layers were chosen to prevent the degradation of QDs in the following fabrication steps, evidenced by a less than 10% drop of the QD emission measured by a microscope (see below).

Then, we mixed SU-8 photoresist with 7 *wt%* of an absorbing dye, Epolight 5820 (Epolin), and spin-coated the mixture on the array as the spectral filter (*ca.* 3.2 μm thick). This filter was then thermally crosslinked at 150 °C for 5 mins, with the regions of blue pixels being opened by a reactive ion etching step (Fig. 1(a)(iv)). The resulting 4-by-4 array had 15 working pixels, with 7 blue and 8 red pixels placed in a mosaic pattern (Fig. 1(b), pixel #11 was lost in array fabrication).

To examine the spectral crosstalk of the array, we analyzed the light intensities of each pixel with an inverted fluorescence microscope (Leica, DMi8). Specifically, the blue [red] light intensity of each pixel was measured with a 400 [565] nm long pass dichroic mirror plus a 460/50 [605/70] nm emission filter, named here as I_{blue} [I_{red}]. The transmission spectra of the spectral filter and the ITO/PMMA stacked layer (spun coated on a separate glass coverslip) were measured with an UV-vis-NIR spectrometer (SHIMADZU 3600). The emission spectra of individual LED pixels were measured by a fiber-coupled spectrometer (OceanOptics, USB2000+).

By sequentially illuminating individual pixels, we measured the optical power and the spatial profile of each pixel with a power meter (Thorlabs PM100D) and an upright microscope (Nikon, FN1), respectively. We next analyzed the microscope image to estimate how much of the measured optical power was within the light spot of each pixel. We then calculated the optical power density of each pixel ($P_{blue/red}$) by dividing the optical power within the light spot by the spot size (95.1 μm^2). Fluorescence images were captured or sampled as we reported before [7].

III. Results and Discussion

We first evaluated the spectral crosstalk in our QD-LED pixels. To do this, we formed ITO/PMMA double layers (via sputtering and spin coating) and the spectral filter (via spin coating) on two separate cover slides, and measured their transmission spectra, respectively. Our data showed that the ITO/PMMA/spectral filter stacking up together yielded an overall transmittance (T%) of *ca.* 4% at 462/19 nm and 84% at 623/45 nm (Fig. 2(a)), which suggested that the ITO/PMMA/spectral filter layers can enhance the wavelength selectivity of red pixels by one order. Correspondingly, we indeed found that the I_{red}/I_{blue} ratios collected at the regions of all 8 red pixels improved from 0.3 to 12 by stacking these three layers on top (Fig. 2(b)), suggesting a dominant red color output with low spectral crosstalk. We noted that QD-LED pixels coated with these ITO/PMMA/spectral filter layers had significantly larger I_{red}/I_{blue} and P_{red} values (see Fig. 3 below) than those coated with distributed Bragg reflector layers (data not shown), suggesting its promise for bi-directional optogenetic studies.

We next confirmed that the emission spectra of individual blue and red pixels (I_{PL}) peaked at *ca.* 462 nm and 623 nm (Fig. 2(c)), respectively, matching the activation spectra of excitatory and inhibitory opsins [2], [3], [9]–[13]. On the other hand, our red pixels did show unwanted light leakage near *ca.* 462 nm, which was most from the 4 neighboring blue pixel regions where the spectral filter was removed. However, the measured P_{blue} values in these 4 regions were as low as 0.01 ± 0.003 mW/mm^2, which will not activate the opsins of interest or cause spectral crosstalk in bi-directional optogenetic studies [9], [11].

To ultimately achieve bi-directional optogenetic control at cellular levels, the light output of a two-color QD-LED array also needs to be high optical power density, localized, and fast-switching, ideally with low electrical power consumption.

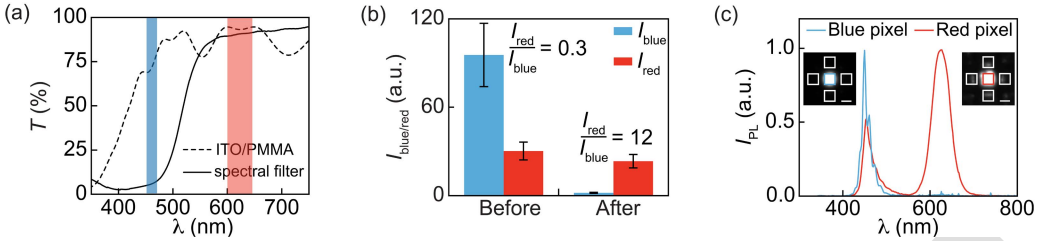

Fig. 2. **Spectral crosstalk of the array.** (a) Transmission spectra of the ITO/PMMA double layers and the spectral filter. Blue and red shaded areas represent the 462/19 nm and 623/45 nm windows, respectively. (b) Averaged $I_{blue/red}$ values from 8 red pixels before and after forming the ITO/PMMA/spectral filter layers on top. All pixels were biased at $I_{LED} = 1$ μA. Error bars represent ± 1 s.d. (c) Emission spectra of a typical blue pixel (pixel #6 in Fig. 1(b)) and a typical red pixel (pixel #7 in Fig. 1(b)). Left (right) insets show bright-field images of the illuminated blue (red) pixels (blue and red squared). White squares mark the regions of four neighboring pixels of the illuminated blue/red pixel. Scale bar, 10 μm.

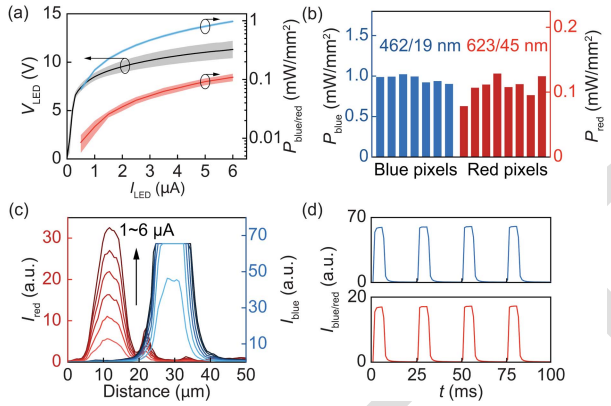

Fig. 3. **Array characterization.** (a) V_{LED} vs I_{LED} (left) and $P_{blue/red}$ vs I_{LED} (right) in both blue and red pixels. Each circle and arrow points to the y-axis corresponding to the respective curve. (b) $P_{blue/red}$ of 7 blue (left) and 8 red (right) pixels. (c) Spatial profile of red pixel #5 and blue pixel #6 in Fig. 1(b) with I_{LED} ranging from 1 to 6 μA. The spatial profile of the blue pixel saturates the microscope camera at $I_{LED} > 1$ μA. (d) Pixel output (blue pixel #9 and red pixel #10 in Fig. 1(b)) pulsed with a 10 ms pulse width at 40 Hz. In (b) and (d), pixels were biased at $I_{LED} = 6$ μA. In (a), shaded areas represent ± 1 s.d.

TABLE I
COMPARISON OF MULTI-COLOR QD-LED ARRAYS

Method	Pitch (μm)	EL/PL	Pixel brightness (cd/m²)	Ref.
Transfer	85 × 230	EL	R/G/B:16380/6425/423	[23]
Ink-jet	254 × 254	EL	R/G/B:352/270/122	[25]
Ink-jet	120 × 330	PL	R:90.38	[26]
Ink-jet	40 × 40	PL	R/G/B: 410/283/229	[27]
Brushing	17 × 17	PL	R/B: 7070/16529	This work

R/G/B: red/green/blue pixels

To this end, we quantified $P_{blue/red}$ at the region of individual pixels across the array. Our data showed that: 1) all 15 pixels increased their $P_{blue/red}$ with the injection current (I_{LED}) ranging from 0.5 to 6 μA (Fig. 3(a)); and 2) when biased at $I_{LED} = 6$ μA, 7 blue pixels had $P_{blue} \sim 0.996 \pm 0.044$ mW/mm^2, whereas 8 red pixels had $P_{red} \sim 0.108 \pm 0.016$ mW/mm^2 (Fig. 3(b)). While pixel-to-pixel variations did exist (e.g. likely due to the amount of filled QDs in SU-8 trenches), it is encouraging to note that the overall high optical power density across the array, $P_{blue} \sim 1$ mW/mm^2 near 462 nm and $P_{red} \sim 0.1$ mW/mm^2 near 623 nm, was sufficient to activate one pair of excitatory and inhibitory opsins (e.g. *ChR2* and *Halo* [2], [3], [9]–[11], *ChRmine* and *Mac* [11]–[13]) for bi-directional optogenetics. Such high $P_{blue/red}$ values were achieved with an electrical power consumption of *ca.* 66 μW (estimated from I-V curves in Fig. 3(a)), suggesting its promise for *in vivo* use [30].

We then moved to analyze the spatial profile of the light spot from each pixel at the surface of the array. The results show that at $I_{LED} = 1 - 6$ μA, both red and blue pixels (e.g., red pixel #5 and blue pixel #6 in Fig.1(b)) output small light spots with their full width at half maximum (FWHM) being *ca.* 10 μm (Fig. 3(c)), the average size of soma in single neurons. This localized light output suggests the promise of our QD-LED array in achieving bi-directional optogenetic control over single cells close to the array surface.

Furthermore, we investigated the switching speed of our QD-LED pixels and found that their localized, high-$P_{blue/red}$ light output can be reliably pulsed at up to 40 Hz with a 10 ms pulse duration (Fig. 3(d)). Each pulse featured *ca.* 2 ms rising and falling times, suitable for temporally precise neurostimulation [31]. These data show that our QD-LED array has sufficient optical power density, spatial resolution, and switching speed for bi-directional optogenetic studies at cellular levels.

Last but not the least, in comparison to other multi-color QD-LED arrays (Table I), our brushing-assisted array featured one order higher pixel brightness than prior ink-jet printing-based arrays [25]–[27], and four-time smaller pitches than prior transfer printing-based arrays [23], suggesting a cost-effective alternative method to build QD-LED arrays.

IV. Conclusion

In sum, we report a 17-μm pitch two-color QD micro-LED array based on brushing-assisted micropatterning of InP/ZnS QDs towards single-cell bi-directional optogenetic studies. After coating the micropatterned QDs with a photoresist-based spectral filter, our resulting QD-LED array was able to output small light spots (*ca.* 10 μm FWHM) with their optical power density being *ca.*1.0 and 0.1 mW/mm^2 near 462 nm and 623 nm, respectively. Combined with its low crosstalk ($I_{red}/I_{blue} > 10$) and fast response (40 Hz), our two-color QD-LED array built from the cost-effective brushing approach may hold promise for enabling bi-directional optogenetics at single-cell levels.

Acknowledgment

The authors thank Amir Arbabi, Yubin Sun, and Tingyi Liu for their technical assistance.

REFERENCES

[1] E. S. Boyden, "Optogenetics and the future of neuroscience," *Nature Neurosci.*, vol. 18, no. 9, pp. 1200–1201, Sep. 2015, doi: 10.1038/nn.4094.

[2] X. Han and E. S. Boyden, "Multiple-color optical activation, silencing, and desynchronization of neural activity, with single-spike temporal resolution," *PLoS ONE*, vol. 2, no. 3, p. e299, Mar. 2007, doi: 10.1371/journal.pone.0000299.

[3] F. Zhang, L.-P. Wang, M. Brauner, J. F. Liewald, K. Kay, N. Watzke, P. G. Wood, E. Bamberg, G. Nagel, A. Gottschalk, and K. Deisseroth, "Multimodal fast optical interrogation of neural circuitry," *Nature*, vol. 446, no. 7136, pp. 633–639, Apr. 2007, doi: 10.1038/nature05744.

[4] M. Kokaia, M. Andersson, and M. Ledri, "An optogenetic approach in epilepsy," *Neuropharmacology*, vol. 69, pp. 89–95, Jun. 2013, doi: 10.1016/j.neuropharm.2012.05.049.

[5] N. Grossman, V. Poher, M. S. Grubb, G. T. Kennedy, K. Nikolic, B. McGovern, R. B. Palmini, Z. Gong, E. M. Drakakis, M. A. A. Neil, M. D. Dawson, J. Burrone, and P. Degenaar, "Multi-site optical excitation using ChR2 and micro-LED array," *J. Neural Eng.*, vol. 7, no. 1, Feb. 2010, Art. no. 016004, doi: 10.1088/1741-2560/7/1/016004.

[6] A. Nakajima, H. Kimura, Y. Sawadsaringkarn, Y. Maezawa, T. Kobayashi, T. Noda, K. Sasagawa, T. Tokuda, Y. Ishikawa, S. Shiosaka, and J. Ohta, "CMOS image sensor integrated with micro-LED and multielectrode arrays for the patterned photostimulation and multichannel recording of neuronal tissue," *Opt. Exp.*, vol. 20, no. 6, p. 6097, Mar. 2012, doi: 10.1364/OE.20.006097.

[7] D. Mao, N. Li, Z. Xiong, Y. Sun, and G. Xu, "Single-cell optogenetic control of calcium signaling with a high-density micro-LED array," *iScience*, vol. 21, pp. 403–412, Nov. 2019, doi: 10.1016/j.isci.2019.10.024.

[8] A. Steude, E. C. Witts, G. B. Miles, and M. C. Gather, "Arrays of microscopic organic LEDs for high-resolution optogenetics," *Sci. Adv.*, vol. 2, no. 5, May 2016, Art. no. e1600061, doi: 10.1126/sciadv.1600061.

[9] N. C. Klapoetke, Y. Murata, S. S. Kim, S. R. Pulver, A. Birdsey-Benson, Y. K. Cho, T. K. Morimoto, A. S. Chuong, E. J. Carpenter, Z. Tian, J. Wang, Y. Xie, Z. Yan, Y. Zhang, B. Y. Chow, B. Surek, M. Melkonian, V. Jayaraman, M. Constantine-Paton, G. K.-S. Wong, and E. S. Boyden, "Independent optical excitation of distinct neural populations," *Nature Methods*, vol. 11, no. 3, pp. 338–346, Mar. 2014, doi: 10.1038/nmeth.2836.

[10] A. S. Chuong, M. L. Miri, V. Busskamp, G. A. C. Matthews, L. C. Acker, A. T. Sørensen, A. Young, N. C. Klapoetke, M. A. Henninger, S. B. Kodandaramaiah, M. Ogawa, S. B. Ramanlal, R. C. Bandler, B. D. Allen, C. R. Forest, B. Y. Chow, X. Han, Y. Lin, K. M. Tye, B. Roska, J. A. Cardin, and E. S. Boyden, "Noninvasive optical inhibition with a red-shifted microbial rhodopsin," *Nature Neurosci.*, vol. 17, no. 8, pp. 1123–1129, Aug. 2014, doi: 10.1038/nn.3752.

[11] J. Mattis, K. M. Tye, E. A. Ferenczi, C. Ramakrishnan, D. J. O'Shea, R. Prakash, L. A. Gunaydin, M. Hyun, L. E. Fenno, V. Gradinaru, O. Yizhar, and K. Deisseroth, "Principles for applying optogenetic tools derived from direct comparative analysis of microbial opsins," *Nature Methods*, vol. 9, no. 2, pp. 159–172, Feb. 2012, doi: 10.1038/nmeth.1808.

[12] H. Marshel, Y. S. Kim, T. A. Machado, S. Quirin, B. Benson, J. Kadmon, C. Raja, A. Chibukhchyan, C. Ramakrishnan, M. Inoue, J. C. Shane, D. J. McKnight, S. Yoshizawa, H. E. Kato, S. Ganguli, and K. Deisseroth, "Cortical layer-specific critical dynamics triggering perception," *Science*, vol. 365, no. 6453, Aug. 2019, Art. no. eaaw5202, doi: 10.1126/science.aaw5202.

[13] B. Y. Chow, X. Han, A. S. Dobry, X. Qian, A. S. Chuong, M. Li, M. A. Henninger, G. M. Belfort, Y. Lin, P. E. Monahan, and E. S. Boyden, "High-performance genetically targetable optical neural silencing by light-driven proton pumps," *Nature*, vol. 463, no. 7277, pp. 98–102, Jan. 2010, doi: 10.1038/nature08652.

[14] Y. Li, J. Tao, Y. Zhao, J. Wang, J. Lv, Y. Qin, J. Liang, and W. Wang, "48 × 48 pixelated addressable full-color micro display based on flip-chip micro LEDs," *Appl. Opt.*, vol. 58, no. 31, p. 8383, Nov. 2019, doi: 10.1364/AO.58.008383.

[15] W.-J. Joo, J. Kyoung, M. Esfandyarpour, S.-H. Lee, H. Koo, S. Song, Y.-N. Kwon, S. H. Song, J. C. Bae, A. Jo, M.-J. Kwon, S. H. Han, S.-H. Kim, S. Hwang, and M. L. Brongersma, "Metasurface-driven OLED displays beyond 10,000 pixels per inch," *Science*, vol. 370, no. 6515, pp. 459–463, Oct. 2020, doi: 10.1126/science.abc8530.

[16] K. Kishino, N. Sakakibara, K. Narita, and T. Oto, "Two-dimensional multicolor (RGBY) integrated nanocolumn micro-LEDs as a fundamental technology of micro-LED display," *Appl. Phys. Exp.*, vol. 13, no. 1, Jan. 2020, Art. no. 014003, doi: 10.7567/1882-0786/ab5ad3.

[17] H.-Y. Lee, Y.-C. Lin, I.-H. Chen, and C.-H. Chao, "Effective color conversion of GaN-based LEDs via coated phosphor layers," *IEEE Photon. Technol. Lett.*, vol. 25, no. 8, pp. 764–767, Apr. 2013, doi: 10.1109/LPT.2013.2250945.

[18] S.-W. Huang Chen, C.-C. Shen, T. Wu, Z.-Y. Liao, L.-F. Chen, J.-R. Zhou, C.-F. Lee, C.-H. Lin, C.-C. Lin, C.-W. Sher, P.-T. Lee, A.-J. Tzou, Z. Chen, and H.-C. Kuo, "Full-color monolithic hybrid quantum dot nanoring micro light-emitting diodes with improved efficiency using atomic layer deposition and nonradiative resonant energy transfer," *Photon. Res.*, vol. 7, no. 4, p. 416, Apr. 2019, doi: 10.1364/PRJ.7.000416.

[19] Z. Liu, C.-H. Lin, B.-R. Hyun, C.-W. Sher, Z. Lv, B. Luo, F. Jiang, T. Wu, C.-H. Ho, H.-C. Kuo, and J.-H. He, "Micro-light-emitting diodes with quantum dots in display technology," *Light, Sci. Appl.*, vol. 9, no. 1, p. 83, Dec. 2020, doi: 10.1038/s41377-020-0268-1.

[20] J. Y. Lin and H. X. Jiang, "Development of microLED," *Appl. Phys. Lett.*, vol. 116, no. 10, Mar. 2020, Art. no. 100502, doi: 10.1063/1.5145201.

[21] Y. Shirasaki, G. J. Supran, M. G. Bawendi, and V. Bulović, "Emergence of colloidal quantum-dot light-emitting technologies," *Nature Photon.*, vol. 7, pp. 13–23, Dec. 2013, doi: 10.1038/nphoton.2012.328.

[22] M. A. Triana, A. A. Restrepo, R. J. Lanzafame, P. Palomaki, and Y. Dong, "Quantum dot light-emitting diodes as light sources in photomedicine: Photodynamic therapy and photobiomodulation," *J. Phys., Mater.*, vol. 3, no. 3, Jun. 2020, Art. no. 032002, doi: 10.1088/2515-7639/ab95e8.

[23] T.-H. Kim, K.-S. Cho, E. K. Lee, S. J. Lee, J. Chae, J. W. Kim, D. H. Kim, J.-Y. Kwon, G. Amaratunga, S. Y. Lee, B. L. Choi, Y. Kuk, J. M. Kim, and K. Kim, "Full-colour quantum dot displays fabricated by transfer printing," *Nature Photon.*, vol. 5, no. 3, pp. 176–182, 2011, doi: 10.1038/nphoton.2011.12.

[24] J.-S. Park, J. Kyhm, H. H. Kim, S. Jeong, J. Kang, S.-E. Lee, K.-T. Lee, K. Park, N. Barange, J. Han, J. D. Song, W. K. Choi, and I. K. Han, "Alternative patterning process for realization of large-area, full-color, active quantum dot display," *Nano Lett.*, vol. 16, no. 11, pp. 6946–6953, Nov. 2016, doi: 10.1021/acs.nanolett.6b03007.

[25] H. M. Haverinen, R. A. Myllyla, and G. E. Jabbour, "Inkjet printed RGB quantum dot-hybrid LED," *J. Display Technol.*, vol. 6, no. 3, pp. 87–89, Mar. 2010, doi: 10.1109/JDT.2009.2039019.

[26] Z. Hu, S. Zhang, W. Peng, S. Zhang, Y. Li, D. Li, S. Jiao, S. Chen, C.-Y. Lee, and H. Zhou, "75-4: Inkjet-printed quantum dot display with blue OLEDs for next generation display," in *SID Symp. Dig. Tech. Pap.*, vol. 50, no. 1, Jun. 2019, pp. 1075–1078, doi: 10.1002/sdtp.13114.

[27] H.-Y. Lin, C.-W. Sher, D.-H. Hsieh, X.-Y. Chen, H.-M.-P. Chen, T.-M. Chen, K.-M. Lau, C.-H. Chen, C.-C. Lin, and H.-C. Kuo, "Optical cross-talk reduction in a quantum-dot-based full-color micro-light-emitting-diode display by a lithographic-fabricated photoresist mold," *Photon. Res.*, vol. 5, no. 5, p. 411, Oct. 2017, doi: 10.1364/PRJ.5.000411.

[28] G.-S. Chen, B.-Y. Wei, C.-T. Lee, and H.-Y. Lee, "Monolithic red/green/blue micro-LEDs with HBR and DBR structures," *IEEE Photon. Technol. Lett.*, vol. 30, no. 3, pp. 262–265, Feb. 1, 2018, doi: 10.1109/LPT.2017.2786737.

[29] E. Jang, S. Jun, H. Jang, J. Lim, B. Kim, and Y. Kim, "White-light-emitting diodes with quantum dot color converters for display backlights," *Adv. Mater.*, vol. 22, no. 28, pp. 3076–3080, Jul. 2010, doi: 10.1002/adma.201000525.

[30] A. H. Marblestone, B. M. Zamft, Y. G. Maguire, M. G. Shapiro, T. R. Cybulski, J. I. Glaser, D. Amodei, P. B. Stranges, R. Kalhor, D. A. Dalrymple, D. Seo, E. Alon, M. M. Maharbiz, J. M. Carmena, J. M. Rabaey, E. S. Boyden, G. M. Church, and K. P. Kording, "Physical principles for scalable neural recording," *Frontiers Comput. Neurosci.*, vol. 7, p. 137, Oct. 2013, doi: 10.3389/fncom.2013.00137.

[31] E. S. Boyden, F. Zhang, E. Bamberg, G. Nagel, and K. Deisseroth, "Millisecond-timescale, genetically targeted optical control of neural activity," *Nature Neurosci.*, vol. 8, pp. 1263–1268, Aug. 2005, doi:10.1038/nn1525.